Please do not adjust margins

This is an Accepted Manuscript of an article published by The Royal Society of Chemistry in Chemical Communications, available online: https://doi.org/10.1039/c9cc02744k

COMMUNICATION

Glass-phase coordination polymer displaying proton conductivity and guest-accessible porosity

Received 00th January 20xx,
Accepted 00th January 20xx

DOI: 10.1039/x0xx00000x

Munehiro Inukai,*[a] Yusuke Nishiyama,[b,c] Kayako Honjo,[d] Chinmoy Das,[e] Susumu Kitagawa,[f] and Satoshi Horike*[d,e,f,g]

We describe the preparation of the crystalline and glassy state of a coordination polymer displaying proton conduction and guest-accessible porosity. EXAFS and solid-state NMR analyses indicated that pyrophosphate and phosphate ions are the main proton transporters in the glass and that homogeneously distributed 5-chloro-1H-benzimidazole in the glass provide the porosity.

Proton-conductive solids are of considerable research interest given their applicability to the membranes of various electrochemical devices such as fuel cells.[1-6] Among these species, those with guest-accessible porosities have attracted much attention recently because the porosity of these solids enhances the conductivity of the materials and their potential use as sensors and catalysts.[7-12] Metal-organic frameworks (MOFs) and coordination polymers (CPs)[13, 14] have recently emerged as interesting classes of proton-conductive solids because of their diverse crystal structures, and reasonably high thermal and chemical stability.[10, 15-18] When mobile proton carriers such as water, azoles, and phosphoric acid are present in the pores and/or within the frameworks of relevant solids, fast proton conduction will be observed. Although some MOFs and CPs with high proton conductivity (above c.a. 10^{-2} S cm^{-1}) have been reported,[19-24] their use as, for example, electrolytes in fuel cells has been limited.[25-27] In fact, improvements with respect to their conductivity, thermal durability, and forming ability are still required for these species to be used in the devices.

Glass-phase CPs obtained by melt-quenching are some of the most attractive species in terms of their ability to form porous materials.[28-34] In contrast to acid treatment, which allows conventional phase-separated porous glass to be obtained, the melt-quenching method can potentially be used to prepare microporous, glass-phase CPs. However, the syntheses and characterizations of glass-phase porous proton-conductive CPs have not been reported. Herein, we report the preparation of a porous CP in crystalline and glassy states, whereby the mentioned glass-phase CP was obtained from the corresponding crystalline state by implementation of the melt-quenching method. The glass-phase material displayed anhydrous proton conductivity and adsorbed water and methanol. The glassy porous CP also showed high proton conductivity under humid conditions because of effective proton transport in the adsorbed water molecules. Extended X-ray absorption fine structure (EXAFS) and solid-state NMR analyses clarified the packing structure and the proton-conduction path.

Crystalline powder sample of CP (hereafter referred to as **1**) was synthesized from ZnO, 5-chloro-1H-benzimidazole (Clbim), and an H_3PO_4 solution (85%) via the liquid-assisted mechanochemical method using methanol. To solve the crystal structure of **1**, we performed single-crystal X-ray diffraction measurements. The structure is two-dimensional (2D) frameworks composed of Zn^{2+}, HPO_4^{2-}, and $H_2PO_4^-$, and three types of uncoordinated guest molecules, namely, protonated Clbim, methanol, and $H_2PO_4^-$ (Fig. 1a). π–π interactions cause the Clbim molecules to be stacked on top of each other at a mutual distance of 3.45 Å. The nitrogen sites of Clbim molecules act as sites of Brønsted basicity and assist the alignment of the hydroxyl groups of guest $H_2PO_4^-$. Four H-bond interactions exist among groups of three adjacent guest $H_2PO_4^-$ species. The O–O

[a] Graduate School of Technology, Industrial and Social Sciences, Tokushima University, 2-1 Minami-Josanjima-Cho, Tokushima 770-8506, Japan
E-mail: inukai.munehiro@tokushima-u.ac.jp
[b] JEOL Resonance Inc., 3-1-2 Musashino, Akishima, Tokyo 196-8558, Japan
[c] NMR Science and Development Division, RIKEN SPring-8 Center, and Nano-Crystallography Unit, RIKEN-JEOL Collaboration Center, Yokohama, Kanagawa 230-0045, Japan
[d] Department of Synthetic Chemistry and Biological Chemistry, Graduate School of Engineering, Kyoto University, Katsura, Nishikyo-ku, Kyoto 615-8510, Japan
[e] AIST-Kyoto University Chemical Energy Materials Open Innovation Laboratory (ChEM-OIL), National Institute of Advanced Industrial Science and Technology (AIST), Yoshida-Honmachi, Sakyo-ku, Kyoto 606-8501, Japan
[f] Institute for Integrated Cell-Material Sciences, Institute for Advanced Study, Kyoto University, Yoshida-Honmachi, Sakyo-ku, Kyoto 606-8501, Japan
[g] Department of Materials Science and Engineering, School of Molecular Science and Engineering, Vidyasirimedhi Institute of Science and Technology, Rayong 21210, Thailand
E-mail: horike@icems.kyoto-u.ac.jp

†Electronic Supplementary Information (ESI) available: Detailed synthetic procedures, XRD, TGA, DSC, adsorption isotherms, solid-state NMR spectra, and crystallographic data. See DOI: 10.1039/x0xx00000x

Please do not adjust margins

Please do not adjust margins

and N–O distances between atoms involved in H-bond interactions are as follows: guest $H_2PO_4^-$–guest $H_2PO_4^-$, guest $H_2PO_4^-$–coordinated HPO_4^{2-}, and $H_2PO_4^-$–Clbim are 2.60 and 2.58 Å (O14H14–O16 and O15H15–O16), 2.68 Å (O12H12–O13), and 2.81 Å (N2H2–O13), respectively (Fig. 1b). The distances are effective from the standpoint of proton conduction based on those of discussion for some representative proton-conductive solids.[35] On the other hand, methanol is surrounded by chloride sites of Clbim and a hydroxyl group of a coordinated HPO_4^-. The distance between the hydroxyl group of HPO_4^- and that of methanol is 2.61 Å (O11–O1S), which indicates the presence of an H-bond between methanol and HPO_4^-. Thermogravimetric analysis (TGA) profile of **1** shows a 3.6% weight loss, which matches well with the loss of methanol (calculated weight loss: 3.6%; Fig. S3). The differential scanning calorimetry (DSC) profile of **1** shows a melting point of 148 °C (Fig. S4a). To obtain the activated **1** (**1a**), **1** was heated at 120 °C under vacuum. The glass-phase derivative of **1** (**1g**) was prepared, in turn, by melt-quenching **1a**. The powder X-ray diffraction (PXRD) pattern of **1a** displays slight differences with respect to that of **1** (Fig. S1), suggesting that only small changes occur in the crystalline structure. The PXRD pattern of **1g** was broadened with respect to that of **1**, suggesting that the structure of the former is amorphous. The DSC profile of **1g** shows a baseline shift at 72 °C, supporting that **1g** is in glassy state (Fig. 1c). We also confirmed the structural transition of **1a** and **1g** at 80 °C under 95% relative humidity (RH) condition. PXRD patterns of **1a** and **1g** changed to another crystal structures (Fig. S1).

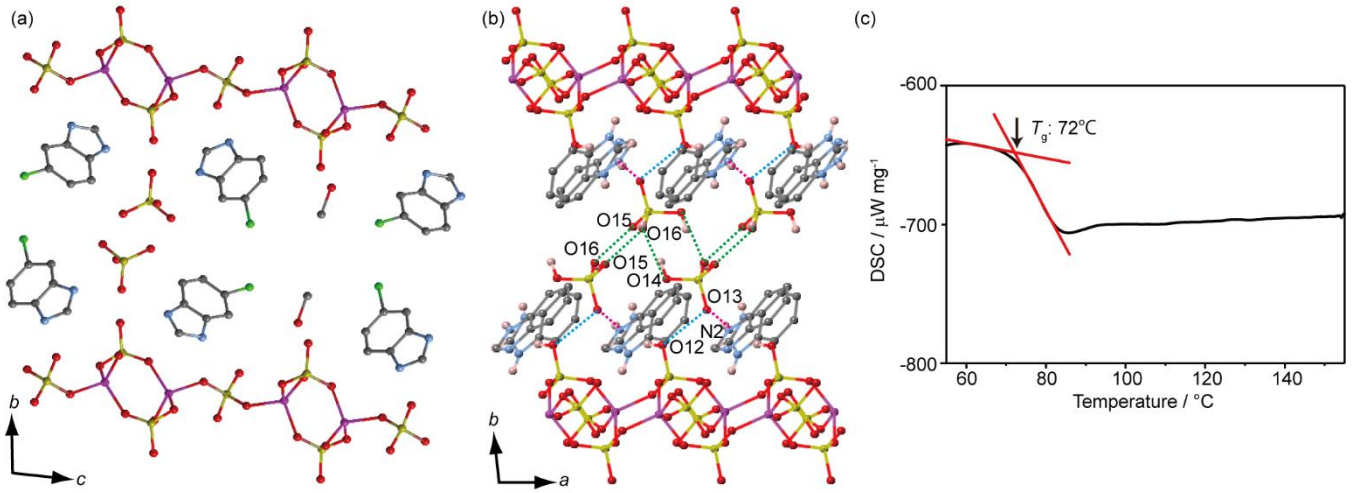

Fig. 1 (a) Crystal structure of $[\{Zn_2(HPO_4)_2(H_2PO_4)\}(ClbimH^+)_2\bullet(H_2PO_4^-)\bullet(MeOH)]_n$ (**1**) viewed along the *a* axis at 223 K. (b) Hydrogen-bond (H-bond) network around guest $H_2PO_4^-$ viewed from the *c* axis. H-bonds between guest $H_2PO_4^-$, guest $H_2PO_4^-$–$ClbimH^+$, and guest $H_2PO_4^-$–coordinated $H_2PO_4^-$ are drawn as green, blue, and pink dotted lines, respectively. (c) Differential scanning calorimetry curve of glass-form **1** (**1g**). [Color coding: purple, Zn; yellow, P; red, O; blue, N; black, C; green, Cl; and light pink, H.]

We measured the water and methanol adsorption isotherms to confirm that the pores in **1a** and **1g** are guest-accessible. The water and methanol adsorption profiles indicate gradual uptakes at 25 °C, suggesting adsorption with the change of structures (gate opening effect).[36-39] Some PXRD peaks due to the 2D frameworks of **1a** change after methanol adsorption, suggesting an increase in the distance between 2D frameworks (Fig. S2). The maximum uptake values of water and methanol were 111.9 and 35.0 mL g^{-1} (4.1 and 1.3 molecules per unit formula), respectively, in the case of **1a** and 118.0 and 61.5 mL g^{-1} (4.3 and 2.3 molecules per unit formula) in the case of **1g** (Figs. 2a and S5). Hysteresis in both isotherms suggests that the hydroxyl groups of the 2D frameworks bind to the adsorbed molecules through H-bonds. **1a** and **1g** were not observed to uptake gases such as N_2 and CO_2. Similarly to previous observations made on a crystalline CP with a dual function,[9] the porosities show specificity for water and methanol.

We performed alternating current impedance measurements to investigate the proton conductivity of **1a** and **1g** (Fig. 2b). In these experiments, **1a** displayed no proton conductivity (< 10^{-9} S cm^{-1}) below 110 °C; however, such conductivity increased linearly in the 115 °C–130 °C, reaching a value of 1.0×10^{-4} S cm^{-1} at 130 °C. Even though the conductivity of **1a** is high at 130 °C, the activation energy of this proton conductor (8.1 eV) is much higher than those of conventional proton-conductive solids (0.1–1.0 eV).[40] In **1a**, the main proton-hopping path would be the one-dimensional guest $H_2PO_4^-$ chain along the *a* axis. Each guest $H_2PO_4^-$ is engaged in multiple H-bond interactions with the adjacent guest $H_2PO_4^-$, Clbim, and coordinated HPO_4^{2-}. These multiple H-bond interactions would hinder the rotation of guest $H_2PO_4^-$, inhibiting proton transport to adjacent guest HPO_4^- and leading to the observed high proton-conduction activation energy. Therefore, **1a** is an example whereby the multiple H-bond interactions established by the uncoordinated phosphates, which are essential to align the phosphate and allow proton transport, induce not only high conductivity but also high activation energy. The encapsulation of phosphate ions in molecules and frameworks is an important theme in the study of biological processes[41, 42] and in the development of proton-conductive solids.[3, 20] The system that we prepared is the first example of a CP comprising aligned uncoordinated phosphates for which proton conduction has been observed. In the case of **1g**, proton conductivity at 130 °C was 1.2×10^{-6} S cm^{-1}, and the activation energy was 1.5 eV. The fact that both conductivity and activation energy were lower in the case of **1g** than in the case of **1a**. It could be due to a smaller

 This journal is © The Royal Society of Chemistry 20xx

Please do not adjust margins

number of H-bond interactions around the phosphate ions, leading to a less effective proton-hopping path. We also measured the proton conductivity of **1a** and **1g** at 25 °C under humid conditions. The CPs displayed no conductivity (**1a** under 95% RH) and 1.2×10^{-4} S cm^{-1} (**1b** under 98% RH; Fig. S6). The high proton conductivity of **1g** would be originated from effective proton transport in the adsorbed water molecules between disordered phosphates and Clbim. The guest-accessible porosity is useful to enhance the conductivity of the glass CP.

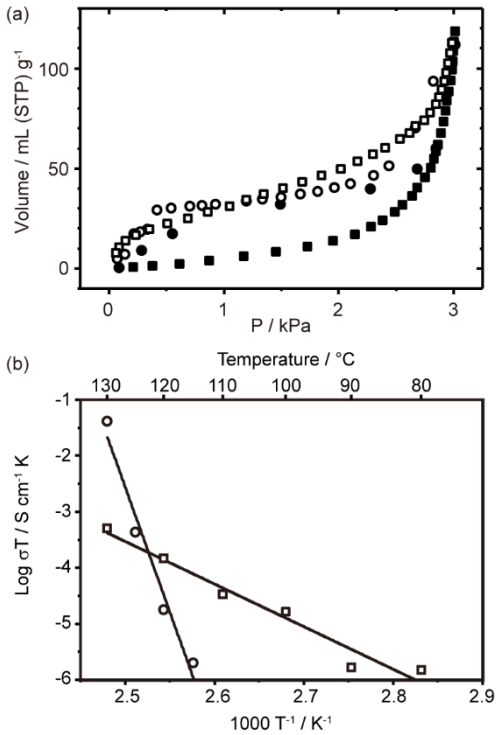

Fig. 2 (a) H_2O adsorption isotherms at 298 K for **1a** (circles) and **1g** (squares). Closed and open circles or squares represent adsorption and desorption, respectively. (b) Arrhenius plots of conductivity of **1a** (circles) and **1g** (squares) under dry N_2 atmosphere.

To investigate the mechanism of proton conduction and the structures of **1a** and **1g**, we conducted EXAFS and solid-state NMR. In particular, the coordination environments and packing structures of the guest molecules were elucidated by EXAFS and solid-state NMR analyses, respectively. All radial distribution functions (RDFs) show a large peak at 1.6–3 Å assigned to the first (Zn–O) and second coordination spheres (Zn–P and Zn–O), as shown in Fig. S7. Although in the case of **1g** the peak intensity decreases as a consequence of the disorder of structure, the peak shapes are almost identical for all three species, suggesting similar coordination environments.

The ^{1}H–^{31}P cross polarization magic angle spinning (CP-MAS) NMR spectrum of **1** is characterized by three peaks due to uncoordinated guest $H_2PO_4^-$ (0 ppm) and coordinated phosphate in the 2D frameworks (Q_0 phosphate, 3.8 and 4.3 ppm; Fig. 3a). The spectrum of **1a** (Fig. 3b) also displays the peak at 0 ppm, indicating that the uncoordinated guest $H_2PO_4^-$ is maintained in the 2D frameworks, even after the material was heated at 120 °C under vacuum. The spectrum of **1g** includes two broad peaks assigned to Q_0 and uncoordinated phosphate at 3.2 ppm and Q_1 phosphate at −8 ppm (Fig. 3c).[43] The appearance of a new peak due to Q_1 would suggest that, during the phase transition from the melting state to glass state, most of two adjacent uncoordinated $H_2PO_4^-$ reacted with each other to form a pyrophosphate ion. The pyrophosphate and the remaining $H_2PO_4^-$ would, in turn, be the main proton transporter in the glassy state frameworks.

The packing structure of Clbim molecules in **1g** was investigated by 2D ^{1}H–^{1}H quantum/single quantum correlation (DQNMR) spectroscopy with ultrafast MAS (MAS is already defined). The spectra reflect the homogenous distribution of Clbim molecules in the 2D frameworks (Fig. S9 and S10). The Clbim molecules and phosphate ions are rearranged within the 2D frameworks during the crystal-to-glass transformation via the molten state. The fact that **1g** has the lower proton conductivity than **1a** are attributed to a decrease in the number of H-bond interactions resulting from the crystal-to-glass transformation. The decrement would induce higher mobility of phosphates, leading to the lower activation energy. With respect to the porosity of **1g**, the homogeneous distribution of Clbim molecules in the 2D frameworks plays a role of pillar molecules, leading to the porosity.

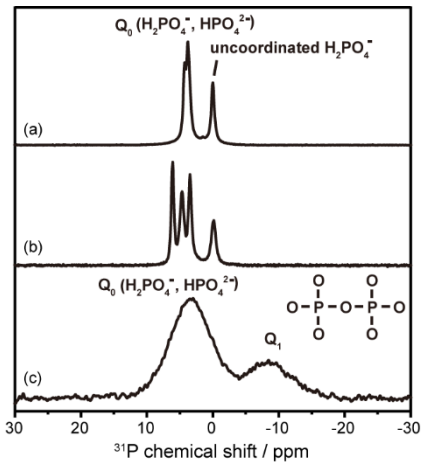

Fig. 3 ^{31}P CP-MAS NMR for (a) **1**, (b) **1a**, (c) **1g** at room temperature.

Conclusions

We synthesized a crystalline porous proton-conductive CP and a glassy state CP by melt-quenching the crystalline CP. The glass-phase CP displayed anhydrous proton conductivity and water- and methanol- accessible porosity. The porosity adsorbing water imparts high proton conductivity to the glass-phase CP. A combination of EXAFS and solid-state NMR analyses allowed us to infer the structure and proton-conduction path of the glass. Clbim acts as a pillar between 2D frameworks and provides the guest-accessible porosity. We believe that the results provide an insight that may aid the development of glassy porous proton-conductive CPs that are potentially useful as membranes in electrochemical devices.

This work was supported by JSPS KAKENHI Grant Number JP17H03043, JP18H02032 and "Molecular Technology'' of

This journal is © The Royal Society of Chemistry 20xx

Please do not adjust margins

Strategic International Collaborative Research Program(SICORP) and Adaptable and Seamless Technology Transfer Program through Target-driven R&D (A-STEP) from the Japan Science and Technology Agency(JST). The EXAFS experiments were conducted at Aichi Synchrotron Radiation Center.

Conflicts of interest

There are no conflicts to declare.

References

1 K.-D. Kreuer, S. J. Paddison, E. Spohr and M. Schuster, *Chem. Rev.*, 2004, **104**, 4637-4678.
2 E. Fabbri, D. Pergolesi and E. Traversa, *Chem. Soc. Rev.*, 2010, **39**, 4355-4369.
3 H. Zhang and P. K. Shen, *Chem. Rev.*, 2012, **112**, 2780-2832.
4 L. Bi, S. Boulfrad and E. Traversa, *Chem. Soc. Rev.*, 2014, **43**, 8255-8270.
5 M. R. Karim, K. Hatakeyama, M. Koinuma and S. Hayami, *J. Mater. Chem. A*, 2017, **5**, 7243-7256.
6 J. Zhang, Y. Xiang, S. Lu and S. P. Jiang, *Adv. Sustainable. Syst.*, 2018, **2**, 1700184.
7 N. C. Jeong, B. Samanta, C. Y. Lee, O. K. Farha and J. T. Hupp, *J. Am. Chem. Soc.*, 2012, **134**, 51-54.
8 B. Scherrer, M. V. F. Schlupp, D. Stender, J. Martynczuk, J. G. Grolig, H. Ma, P. Kocher, T. Lippert, M. Prestat and L. J. Gauckler, *Adv. Funct. Mater.*, 2013, **23**, 1957-1964.
9 D. Umeyama, S. Horike, M. Inukai and S. Kitagawa, *J. Am. Chem. Soc.*, 2013, **135**, 11345-11350.
10 X. Meng, H.-N. Wang, S.-Y. Song and H.-J. Zhang, *Chem. Soc. Rev.*, 2017, **46**, 464-480.
11 S. Ø. Stub, E. Vøllestad and T. Norby, *J. Mater. Chem. A*, 2018, **6**, 8265-8270.
12 S.-S. Bao, G. K. H. Shimizu and L.-M. Zheng, *Coord. Chem. Rev.*, 2019, **378**, 577-594.
13 O. M. Yaghi, M. O'Keeffe, N. W. Ockwig, H. K. Chae, M. Eddaoudi and J. Kim, *Nature*, 2003, **423**, 705-714.
14 S. Kitagawa, R. Kitaura and S.-i. Noro, *Angew. Chem. Int. Ed.*, 2004, **43**, 2334-2375.
15 M. Yoon, K. Suh, S. Natarajan and K. Kim, *Angew. Chem. Int. Ed.*, 2013, **52**, 2688-2700.
16 S. Horike, D. Umeyama and S. Kitagawa, *Acc. Chem. Res.*, 2013, **46**, 2376-2384.
17 T. Yamada, K. Otsubo, R. Makiura and H. Kitagawa, *Chem. Soc. Rev.*, 2013, **42**, 6655-6669.
18 P. Ramaswamy, N. E. Wong and G. K. H. Shimizu, *Chem. Soc. Rev.*, 2014, **43**, 5913-5932.
19 M. Sadakiyo, T. Yamada and H. Kitagawa, *J. Am. Chem. Soc.*, 2009, **131**, 9906-9907.
20 V. G. Ponomareva, K. A. Kovalenko, A. P. Chupakhin, D. N. Dybtsev, E. S. Shutova and V. P. Fedin, *J. Am. Chem. Soc.*, 2012, **134**, 15640-15643.
21 S. S. Nagarkar, S. M. Unni, A. Sharma, S. Kurungot and S. K. Ghosh, *Angew. Chem. Int. Ed.*, 2014, **53**, 2638-2642.
22 S. Kim, K. W. Dawson, B. S. Gelfand, J. M. Taylor and G. K. H. Shimizu, *J. Am. Chem. Soc.*, 2013, **135**, 963-966.
23 N. T. T. Nguyen, H. Furukawa, F. Gándara, C. A. Trickett, H. M. Jeong, K. E. Cordova and O. M. Yaghi, *J. Am. Chem. Soc.*, 2015, **137**, 15394-15397.
24 Y. Ye, W. Guo, L. Wang, Z. Li, Z. Song, J. Chen, Z. Zhang, S. Xiang and B. Chen, *J. Am. Chem. Soc.*, 2017, **139**, 15604-15607.
25 H. B. Aiyappa, S. Saha, P. Wadge, R. Banerjee and S. Kurungot, *Chem. Sci.*, 2015, **6**, 603-607.
26 M. Inukai, S. Horike, T. Itakura, R. Shinozaki, N. Ogiwara, D. Umeyama, S. Nagarkar, Y. Nishiyama, M. Malon, A. Hayashi, T. Ohhara, R. Kiyanagi and S. Kitagawa, *J. Am. Chem. Soc.*, 2016, **138**, 8505-8511.
27 D. Gui, X. Dai, Z. Tao, T. Zheng, X. Wang, M. A. Silver, J. Shu, L. Chen, Y. Wang, T. Zhang, J. Xie, L. Zou, Y. Xia, J. Zhang, J. Zhang, L. Zhao, J. Diwu, R. Zhou, Z. Chai and S. Wang, *J. Am. Chem. Soc.*, 2018, **140**, 6146-6155.
28 D. Umeyama, S. Horike, M. Inukai, T. Itakura and S. Kitagawa, *J. Am. Chem. Soc.*, 2015, **137**, 864-870.
29 T. D. Bennett, Y. Yue, P. Li, A. Qiao, H. Tao, N. G. Greaves, T. Richards, G. I. Lampronti, S. A. T. Redfern, F. Blanc, O. K. Farha, J. T. Hupp, A. K. Cheetham and D. A. Keen, *J. Am. Chem. Soc.*, 2016, **138**, 3484-3492.
30 W. Chen, S. Horike, D. Umeyama, N. Ogiwara, T. Itakura, C. Tassel, Y. Goto, H. Kageyama and S. Kitagawa, *Angew. Chem. Int. Ed.*, 2016, **55**, 5195-5200.
31 H. Tao, T. D. Bennett and Y. Yue, *Adv. Mater.*, 2017, **29**, 1601705.
32 S. S. Nagarkar, S. Horike, T. Itakura, B. Le Ouay, A. Demessence, M. Tsujimoto and S. Kitagawa, *Angew. Chem. Int. Ed.*, 2017, **56**, 4976-4981.
33 A. Qiao, T. D. Bennett, H. Tao, A. Krajnc, G. Mali, C. M. Doherty, A. W. Thornton, J. C. Mauro, G. N. Greaves and Y. Yue, *Sci. Adv.*, 2018, **4**, eaao6827.
34 C. Zhou, L. Longley, A. Krajnc, G. J. Smales, A. Qiao, I. Erucar, C. M. Doherty, A. W. Thornton, A. J. Hill, C. W. Ashling, O. T. Qazvini, S. J. Lee, P. A. Chater, N. J. Terrill, A. J. Smith, Y. Yue, G. Mali, D. A. Keen, S. G. Telfer and T. D. Bennett, *Nat. Commun.*, 2018, **9**, 5042.
35 S. J. Paddison, K.-D. Kreuer and J. Maier, *Phys. Chem. Chem. Phys.*, 2006, **8**, 4530-4542.
36 R. Kitaura, K. Fujimoto, S.-i. Noro, M. Kondo and S. Kitagawa, *Angew. Chem. Int. Ed.*, 2002, **41**, 133-135.
37 J.-R. Li, R. J. Kuppler and H.-C. Zhou, *Chem. Soc. Rev.*, 2009, **38**, 1477-1504.
38 A. Schneemann, V. Bon, I. Schwedler, I. Senkovska, S. Kaskel and R. A. Fischer, *Chem. Soc. Rev.*, 2014, **43**, 6062-6096.
39 Z. Chang, D. H. Yang, J. Xu, T. L. Hu and X. H. Bu, *Adv. Mater.*, 2015, **27**, 5432-5441.
40 K.-D. Kreuer, *Chem. Mater.*, 1996, **8**, 610-641.
41 P. D. Beer and P. A. Gale, *Angew. Chem. Int. Ed.*, 2001, **40**, 486-516.
42 P. S. Lakshminarayanan, I. Ravikumar, E. Suresh and P. Ghosh, *Chem. Commun.*, 2007, 5214-5216.
43 K. J. D. Mackenzie and M. E. Smith, *Multinuclear Solid-State Nuclear Magnetic Resonance of Inorganic Materials*, Pergamon, 2002.

 This journal is © The Royal Society of Chemistry 20xx

Please do not adjust margins